Chapter 13

A Passively Stable Hovering Flapping Micro-Air Vehicle

Floris van Breugel, Zhi Ern Teoh, and Hod Lipson

Abstract Many insects and some birds can hover in place using flapping wing motion. Although this ability is key to making small scale aircraft, hovering flapping behavior has been difficult to reproduce artificially due to the challenging stability, power, and aeroelastic phenomena involved. A number of ornithopters have been demonstrated, some even as toys, nearly all of these designs, however, cannot hover in place because lift is maintained through airfoils that require forward motion. Two recent projects, DeLaurier's Mentor Project and the TU Delft's DelFly (Chapter 14), have demonstrated flapping based hovering flight. In an effort to push the field forward even further, we present here the first passively stable 24 g hoverer capable of hovering flapping flight at a Reynolds number similar to insects ($Re = 8{,}000$). The machine takes advantage of the clap and fling effect, in addition to passive wing bending to simplify the design and enhance performance. We hope that this will aid in the future design of smaller machines, and shed light on the mechanisms underlying insect flight.

13.1 Introduction

In this chapter we will discuss the design and fabrication of a passively stable hovering flapping machine. This work is motivated by the unmatched aerodynamic ability of insects and hummingbirds to hover in place in addition to other acrobatic feats such as flying backward and sideway by exploiting flapping wing motion [5]. Although this remarkable ability is key to making small-scale aircraft, flapping-hovering behavior has been difficult to reproduce artificially due to the challenging stability, power, and aeroelastic phenomena involved. Recent interest in small-scale unmanned air vehicles, especially those capable of hovering like insects and hummingbirds, is driven by many potential applications ranging from surveillance and exploration to flocks of rapidly reconfigurable 3-D airborne machines. A working robotic model of flapping flight is also of interest to biologists and fluid dynamicists for better understanding the dynamics governing flapping flying organisms.

A number of flapping machines have been developed [13, 17, 12, 11, 21, 1, 3], but few are capable of untethered hovering flight [16, 6]. A key challenge is to demonstrate stable untethered hovering flapping ability at a weight and power approximating that of insects and birds where hovering flapping flight is observed in nature. In this chapter we will discuss the recent development of a passively stable 24 g machine capable of hovering flapping flight at a Reynolds number similar to insects ($Re = 8{,}000$). This design, particularly the passive stability, may help in the design of insect-sized hovering vehicles, as well as shed light on the aeroelastic dynamic principles underlying insect flight.

For the past several decades researchers have been studying how the complex flows form that allow insects to perform such incredible aerial feats, and what effect they have on flight at small scales with the hope of building a fly-sized hovering flapping machine. Flapping flight, such as that employed by insects, offers several advantages over ornithoptic flapping flight as seen in larger birds (i.e., incapable of

F. van Breugel (✉)
Cornell Computational Synthesis Lab, Cornell University, Ithaca, New York, USA
e-mail: fv28@cornell.edu

D. Floreano et al. (eds.), *Flying Insects and Robots*,
DOI 10.1007/978-3-540-89393-6_13,

hovering) or fixed and rotary wing flight, most notably in scalability to small sizes [9]. At smaller sizes, such as that of a fruit fly, fixed wing airfoils become less efficient than flapping flight due to the low Reynolds number. Low Reynolds numbers also appear in thin atmospheres such as that found on Mars [18], where conventional airborne exploration would be difficult. While some research suggests that flapping flight is more efficient than both translational and spinning wing flight [20], it is still debatable whether flapping or spinning wings are most efficient at small scales. It is clear from insect flight, however, that flapping wings allow for robust efficient, and incredibly maneuverable flight, and should thus be considered as a potential approach to MAV design.

Current work has focused on thrust mechanisms that produce sufficient lift for hovering flight, and that provide a future of possible methods for control. Recent advances in small motors and batteries made by the cellphone industry have made miniature lightweight robotics much more feasible. Significant work has been done on forward flying flapping micro-air vehicles, but these cannot hover. Two micro-air vehicles have demonstrated hovering abilities, most notably SRI/UTIAS and Delauriers Mentor project [6], and the DelFly 2 from TU Delft and Wageningen University (Chap. 14) [16]. Both of these machines take advantage of opposing wing pairs flapping together and rely on conventional rudders for control. Fearing and Wood [11] have recently demonstrated a fly-sized flapping machine takeoff, but used off-board power and stabilization. The design presented here offers a scalable flapping wing architecture that provides the opportunity for quad-rotor-like active control using flapping wing pairs rather than conventional rudders for control. We further demonstrate that the machine is passively stable, thus eliminating the need for active stabilization control, a property which may help eliminate the need for complex and relatively heavy active stabilization systems in smaller scale future designs.

13.2 Aerodynamics of Flapping Flight

The key to building a flapping-hovering machine is understanding the aerodynamic forces involved, as well as the wing motions and aeroelastic dynamics required to generate those forces. It has long been established that there must be fluid–wing interactions beyond traditional aerodynamic theory that accounts for insects ability to actually fly [10]. Scientists have been working on understanding the complex unsteady aerodynamic flows that form in the intermediate Reynolds numbers between 10^1 and 10^4, where insect flight generally falls [19]. Several other chapters in this book cover the aerodynamics in great detail, thus we will only provide a brief overview of the aerodynamic flows here.

The precise mechanism that forms and utilizes the complex flows that make insect flight possible is still an active research area, but the underlying theories to explain the phenomena have come a long way. The first unsteady aerodynamic effect proposed to explain lift enhancement in insects is the Weis-Fogh clap and fling effect, which has been described in detail using both insects and robotic setups [15]. As the wings start to peel apart at the beginning of the fling phase (outstroke), a low-pressure region forms that pulls air into the cleft around the leading edge (Fig. 13.1). This influx of air strengthens the formation of the leading edge vortices, which increases the circulation and thus lift. A similar mechanism, though less pronounced, takes place on the clap, where the air leaving the gap between the two wings helps increase vortex formation [15]. In nature most insects do not rely on this mechanism for the majority of their flight strokes as it can be very damaging to the wings. It has, however, been a strong motivation for the design of a number of flapping wing vehicles, including the Mentor project, the DelFly (Chap. 14), Dr. Jones' flapping machine (Chap. 12), and the machine discussed in this chapter.

In addition, three more general mechanisms for lift enhancement beyond traditional aerodynamic theory have been established: delayed stall, rotational circulation, and wake capture [7]. Delayed stall is a translational mechanism by which leading edge vortices are formed, resulting in a higher circulation about the wing, increasing net lift. Rotational circulation is an inviscid mechanism representing the circulation needed to satisfy the Kutta condition at the trailing edge due to the upwash/downwash cause by the wing rotation. Wake capture is a gust response to the wake flow patterns whereby the wings recapture the wake from the previous half stroke on their return, taking advantage of the energy already spent to generate the vortex wake [7].

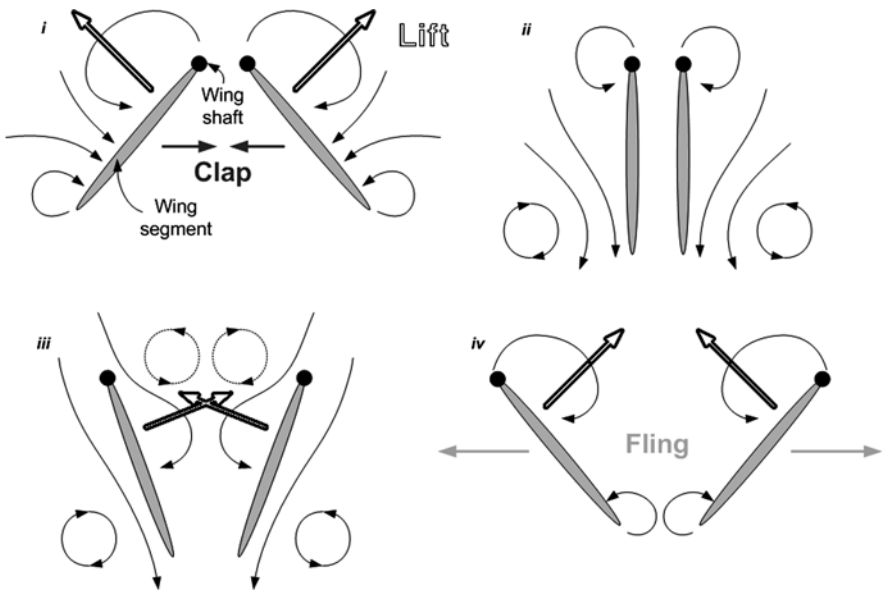

Fig. 13.1 Diagram depicting vortex formation and shedding throughout the cycle (adapted from Lehmann, Sane, & Dickinson, 2005). As the wings come together (i) vortices are formed at the trailing and leading edges, these are then shed (ii) and recaptured during the fling phase (iii). This mechanism provides a substantial increase in lift production

13.2.1 Passive Wing Pitching

An important factor in controlling the formation of these aerodynamic processes and utilizing them is precise control of the wing. Using a robotic setup, Dickinson proposed that by carefully controlling the timing of the wing pitch and delayed stall the insect could theoretically increase their lift by 35% during peaks [7], but this comes at a cost of increased drag and reduced efficiency [19]. Recent work on insect flight dynamics has shown that energy efficiency is improved through the use of wing dynamics to help pitch the wing [2]. Studies on the hawkmoth have shown that wing bending is even largely independent of fluid dynamics, suggesting that complex stroke patterns can be designed purely through wing architecture and careful design of the wings moment of inertia [4]. Further work on *Drosophila* wing stroke patterns has shown that it is likely that the majority of the pitching occurs passively [8]. Nearly all successful small-scale flapping-based machines that have been demonstrated have made use of aeroelastic pitching, either through baggy wing skins or an elastic skeleton [13, 17, 12, 11, 21, 1, 3, 16, 6].

Using such a passive mechanism to control the wing motion drastically reduces the complexity of the design by eliminating the need for a second actuator to actively control the wing pitch. A single actuator can be used to flap the wings, while a combination of air drag and the wings moment of inertia and elasticity bends the wing plane such that it provides a positive lift force on both the in-and outstrokes. The timing of the rotation, extent to which the wings bend, and thus the lift coefficient are controlled by the material properties of the wings. This aeroelastic bending is shown in Fig. 13.2.

13.3 Machine Design

With the natural inspirations from insect and hummingbird flight in mind, we set about designing a small hovering flapping machine. The design principle was to combine a number of modules each consisting of a DC motor and a pair of flapping wings, based on insect and hummingbird flight. Note that the wings needed to be configured such that they provided vertical thrust, rather than lateral thrust as in an ornithopter, which requires an airfoil to generate lift from forward flight. The first design, pictured in Fig. 13.3, consisted of three such modules. In later designs we began using four modules for several reasons. While this project did not make use of any active control, the presence of four independent motor–wing pairs allows for the potential of actively controlled flight. Also, adding an additional module increased the net lifting power of the machine, and simplified the angles in the modules' chassis. The

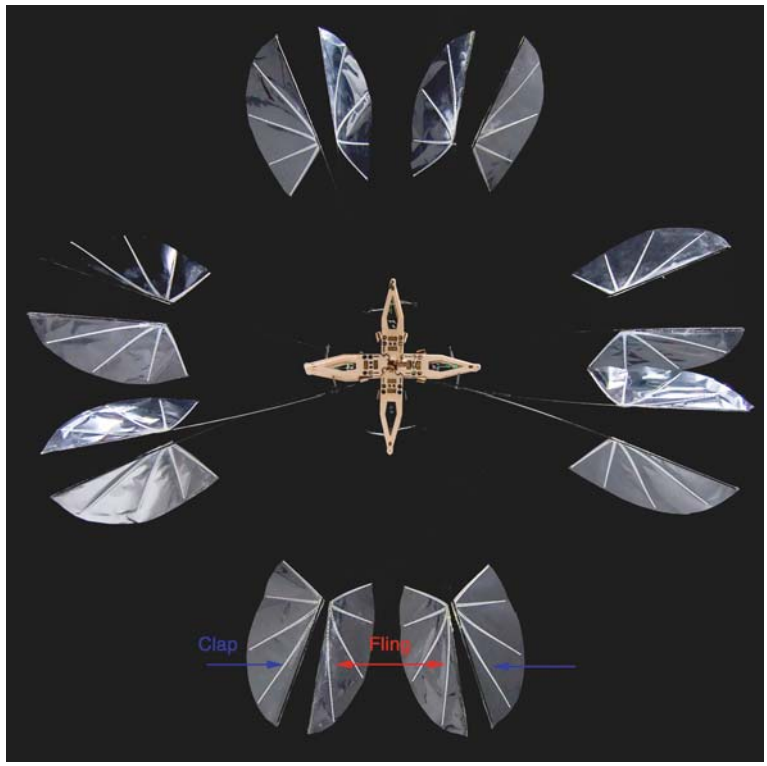

Fig. 13.2 Aeroelastic wing bending. Machine shown under a strobe light during flapping at 20 Hz. The image is composed of several individual images to show both the instroke and outstroke of each wing pair. The inner pair is the outstroke, the outer pair the instroke. Air drag bends the wings, providing an appropriate angle of attack, allowing for positive lift generation throughout the entire cycle. The fluid inertia combined with the slowing down and switching direction passively pitches the wings. Similar mechanisms for wing control have been observed in insects

final design, capable of untethered hovering flapping flight, is the version discussed here in more detail.

We have designed an 18 g machine (excluding batteries, 24 g including batteries) capable of hovering flapping flight, see Fig. 13.4. The design consists of four pairs of wings; each independently powered by a small DC motor and designed to act in a similar manner to an insect, taking advantage of passive wing bending, the clap-and-fling effect, as well as the other unsteady aerodynamic effects, with a single active

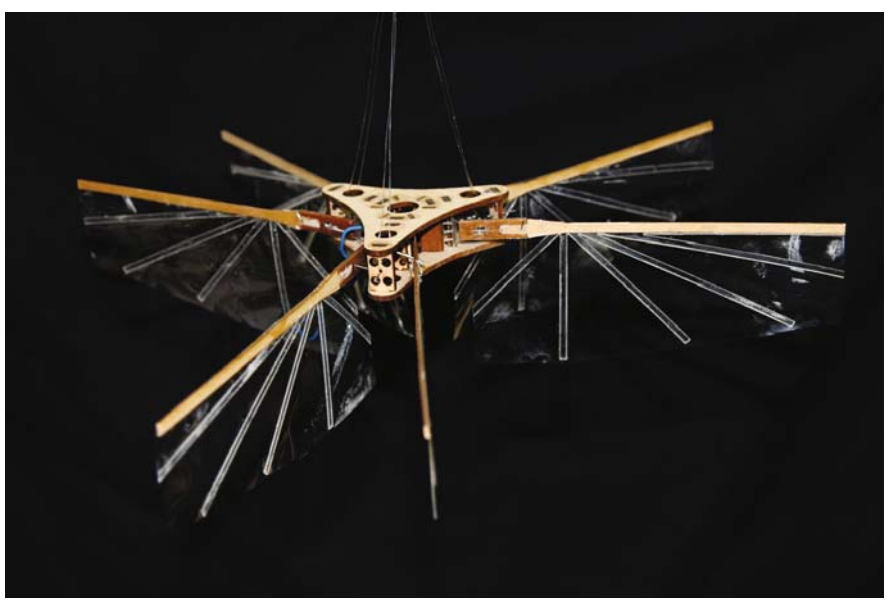

Fig. 13.3 Initial design of hovering flapping machine. Theoretically this three-winged version should be equally capable of being passively stable as our more successful four-winged version. We moved to four-wings primarily to simplify the design of the angles in the modules' chassis and allow for a potential future of active control

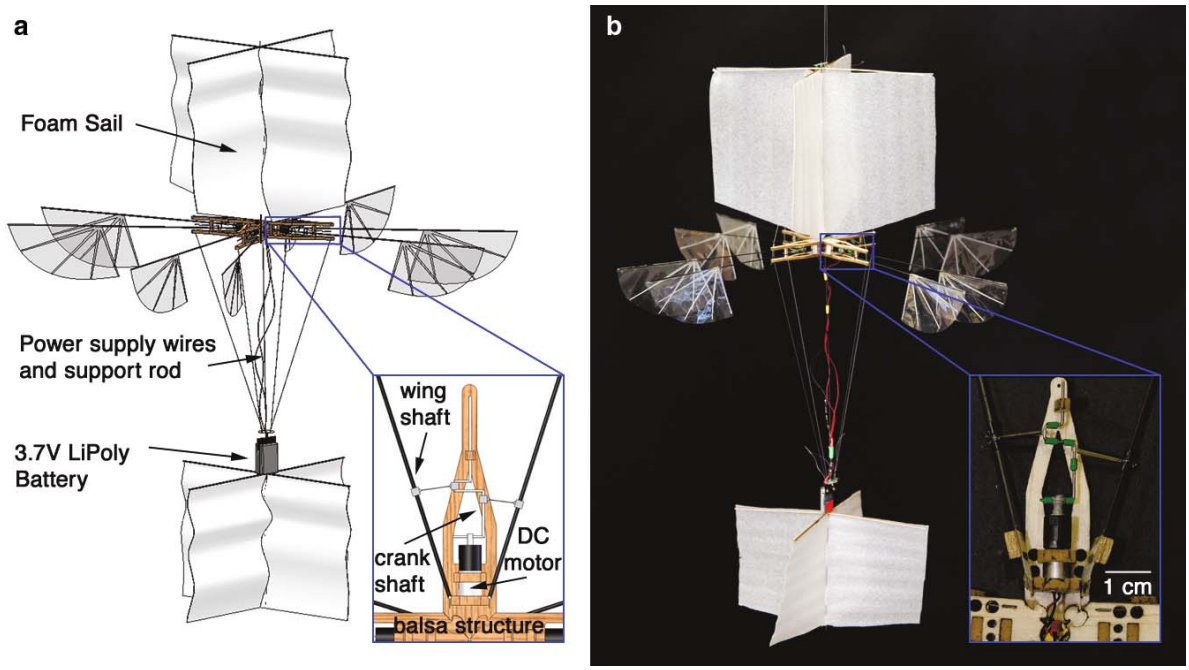

Fig. 13.4 Design and material properties: (**a**) solidworks designed CAD model and. (**b**) physical machine. The DC motor is connected to the wing shafts with a crankshaft and connecting rods. As the crankshaft turns the wings flap in and out, nearly symmetrically. Opposite wing pairs are reversed to reduce effects of the slight asymmetry

degree of freedom. The machine we present here is entirely passively stabilized (Fig. 13.3), yet the presence of four independent pairs allows for future implementation of active control. In this section we discuss a general approach to building small-scale lightweight machines using simple manufacturing techniques. As with any airborne vehicle, weight is of critical importance, and particular attention should be paid to material selection and component design in order to remove unnecessary weight.

Balsa wood has a very high strength to weight ratio and is easy to work with, making it the perfect material for structural components. In order to maximize the strength of balsa it is critical to use the wood grain to your advantage, which we were able to do by virtue of our modular design. Each module was cut such that the grain went with the longest (most fragile) dimension. Balsa also comes in a variety of grades which differ significantly in strength and density. Complicated structures can easily be cut out and etched into the wood using a laser cutter, such as that available from Epilog (http://www.epiloglaser.com/). For our machine's structural components we used 2.4 mm (3/32 in.) balsa sheets laser-cut into interlocking components to take advantage of the wood grain.

As discussed earlier, flexible wings are key. After much experimentation we found that wings comprised a 13 μm PET (polyethylene terephthalate) film welded (using a soldering iron) to a laser-cut vein pattern made of 250 μm PET worked particularly well. Wing pairs were attached to the flapping mechanism using 21 cm long, 0.9 mm diameter carbon fiber rods. The flexible carbon fiber allows the wings to twist, providing additional feathering as well as providing some energy storage through wing bending, increasing the amplitude of the flap. Wing shafts were connected to the structure with a PET flexible hinge joint to constrain motion to the desired plane. Minimum distance between static wings was designed to be 0.2 of the chord length, to maximize the benefits from clap and fling effect. Flapping motion of each wing pair was generated by a separate 1.2 g geared (25:1) DC pager motor (GM15, distributed through Solarbotics, Calgary, CN). The motor turned a hand-bent 0.6 mm diameter steel crankshaft, which was connected to the wings with connecting rods and ball joints (steel tube and fishing line knots on either end). Motors were powered in parallel by two 3.1 g, 3.7 V, 90 mAh Li-Poly batteries in series (available through plantraco.com). Batteries were connected to the structure with a 24 cm

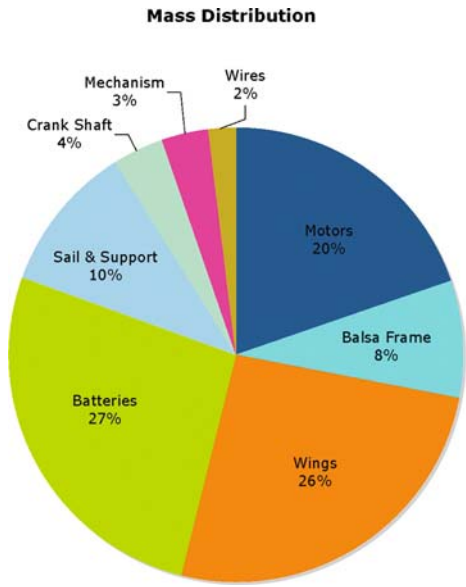

Part	Mass (g)	Quantity	Subtotal
Motors	1.2	4	4.8
Balsa Frame	0.5	4	2
Wings	0.78	8	6.24
Batteries	3.25	2	6.5
Sail & Support	2.5	1	2.5
Crank Shaft	0.22	4	0.88
Mechanism	0.2	4	0.8
Wires	0.5	1	0.5
		Total (g)	24.22

Fig. 13.5 Mass distribution of parts

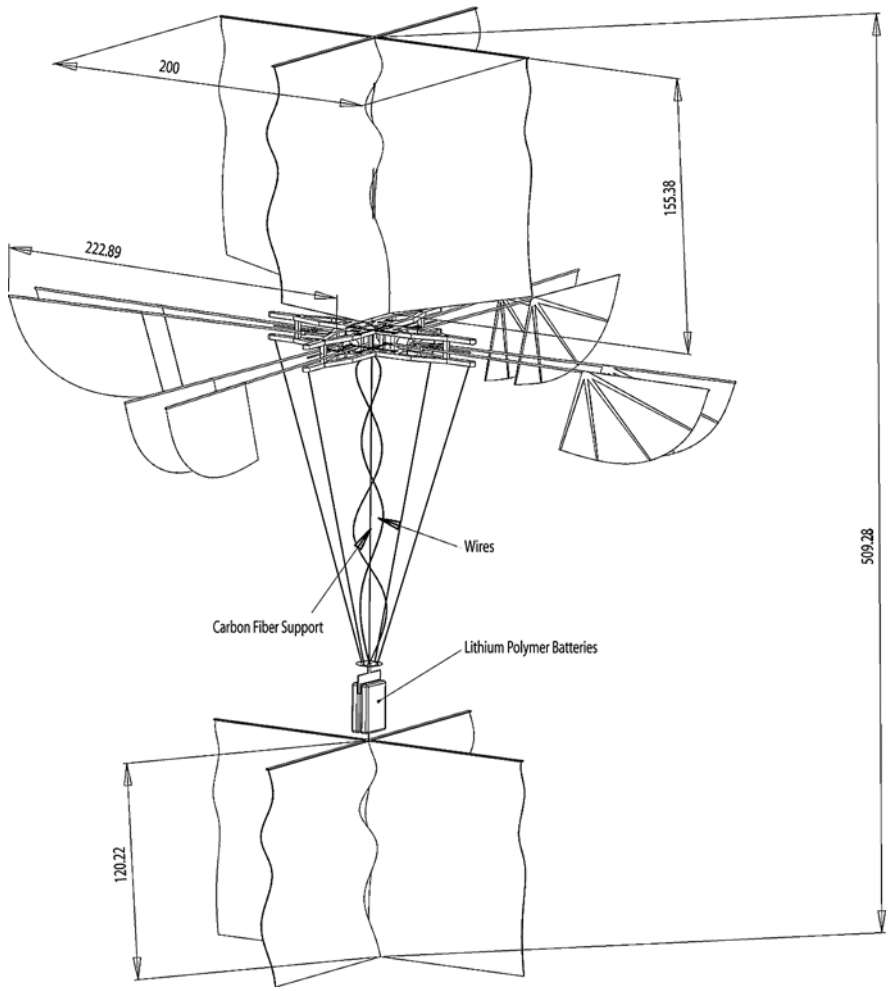

Fig. 13.6 Dimensioned drawing of full model, dimensions in mm

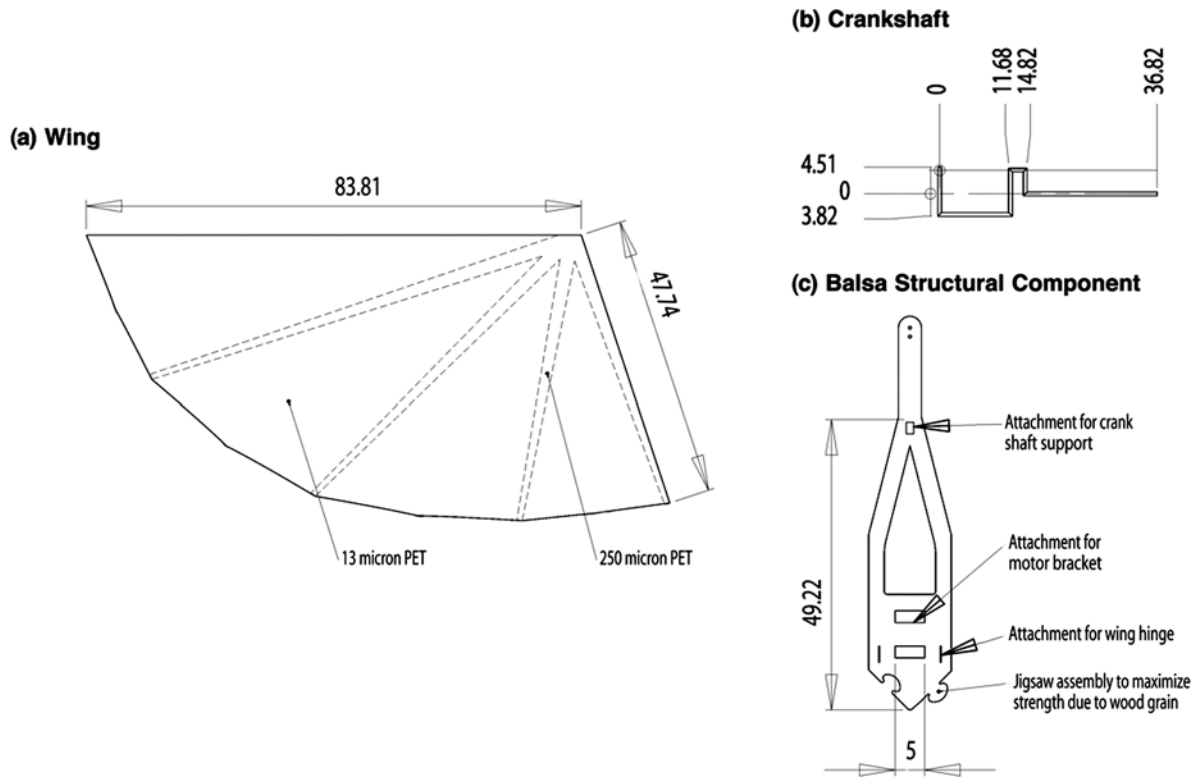

Fig. 13.7 Dimensioned critical components, dimensions in mm

long, 0.4 mm steel rod, reinforced by 0.2 mm fishing line to ensure rigidity. (Later the steel rod and fishing line were replaced with a 0.9 carbon fiber rod, which provided sufficient rigidity at a lower weight.) Top and bottom sails were constructed from lightweight semi-rigid packing foam, reinforced by balsa struts at the top. Total weight of the machine including sails and both batteries was 24.2 g (see Figs. 13.4 and 13.5). In an effort to promote research in the area of small-scale hovering flapping machines we include here the precise blueprints of our design to aid in others' construction of such robots, see Figs. 13.6 and 13.7 (for more details contact authors).

13.3.1 Design Improvements

Since building and testing the machine presented in the previous section we have made a number of changes to improve the design; here, we discuss some of these changes and potential future changes as well. Occasionally the jigsaw fittings on the modular design presented a problem, either through fragility or fatigue due to vibrations. In order to fix this we tested a variety of different material approaches including composites and other balsa designs. Composites proved difficult to use as they were significantly heavier than their balsa counterparts, and also made it much more difficult to take the machine apart and replace parts such as motors. Thus, a new way of joining the four modules is shown in Fig. 13.8. A module connector is used to secure both the top and bottom of each module and is also used to connect all four modules together. Span-wise connector arms are used to connect the modules to the module connector. Initially, length-wise connector arms were used but when built, flapping caused excessive vibrations. The span-wise connector arms reduced the vibrations significantly. Using a module connector enables individual modules to be built and then assembled. In the event that module 1 has a faulty motor, only module 1 would be affected leaving the modules 2, 3, and 4 free from damage. The modules are made of 1/16 in. balsa, while the module connector and the connector arms are made of 3/32 in. balsa wood.

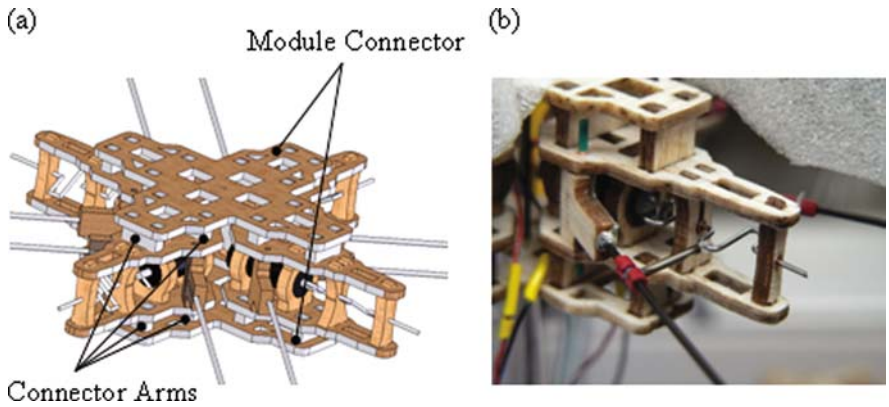

Fig. 13.8 (**a**) Solidworks designed CAD model of module connector. (**b**) Physical machine. The *top* and *bottom* module connectors provide the rigidity needed when the wings flap

The next improvement we made was to redesign the crankshaft. The original crankshaft placed the wing load directly on the DC motor via the crankshaft. In the new design a second bearing was introduced between the attachment to the wings and the DC motor, relieving the motor from the direct loading. Additionally some changes had to be made to the balsa structure, as seen in Fig. 13.9.

Lastly, we updated the PET flexible hinge in order to reduce losses in the system. The original flexible hinge introduced more damping than necessary, and was thus replaced with a pinned hinge to allow for free rotation as shown in Fig. 13.10 a–d, which shows the actual redesign of the hinge and its ease of assembly. Currently, the pins used are 0.026 in. steel music wire. To decrease weight, carbon fiber rods of similar dimensions could be used instead. The hinge was fabricated by combining etching and vector laser cutting 3/32 in. balsa wood. A groove for the pin slot was etched and the shape of the hinge was vector cut. The pinned hinge will also make it easier to install and uninstall the wings for repair or modifications.

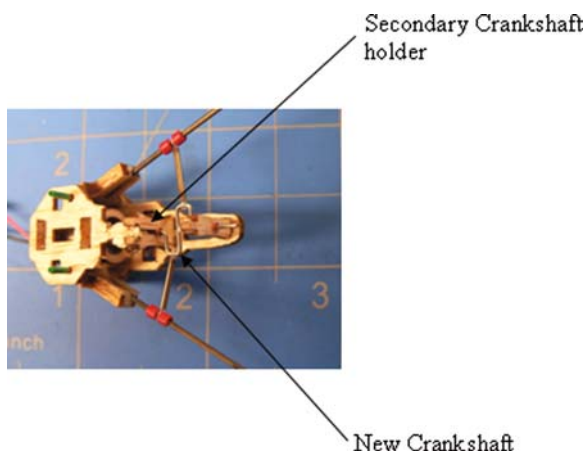

Fig. 13.9 New design of the crankshaft. The frame was redesigned to accommodate the secondary crankshaft holder

13.4 Passive Stability

Hovering flapping-based flying machines are notoriously unstable, and generally require a suite of sensors and processing power to maintain stability or constant manual remote control. Note the distinction between hovering flight and forward flight, as there have been countless stable forward-flying ornithopters. Adding the necessary sensors and processors on board is often impossible for smaller vehicles due to weight limitations, making untethered automatic control extremely difficult if not impossible. In this section we discuss an alternative to active control: passive stability through the use of strategically placed dampers. This approach can be valuable for testing the propulsion systems, and to a certain extent to compliment active control by reducing the need for precision.

From a control's perspective, our machine's architecture is similar to that of a quad-rotor and could theoretically be controlled in much the same manner if outfitted with accelerometers, gyros, a microcontroller, and speed controllers. Rather than implementing such an active control system, however, we opted to explore passive stability. The physical control concepts presented here could theoretically be converted to gains for a classical PID controller using electronics rather than sails for control. The passive mechanism we used is likely not applicable to situations where

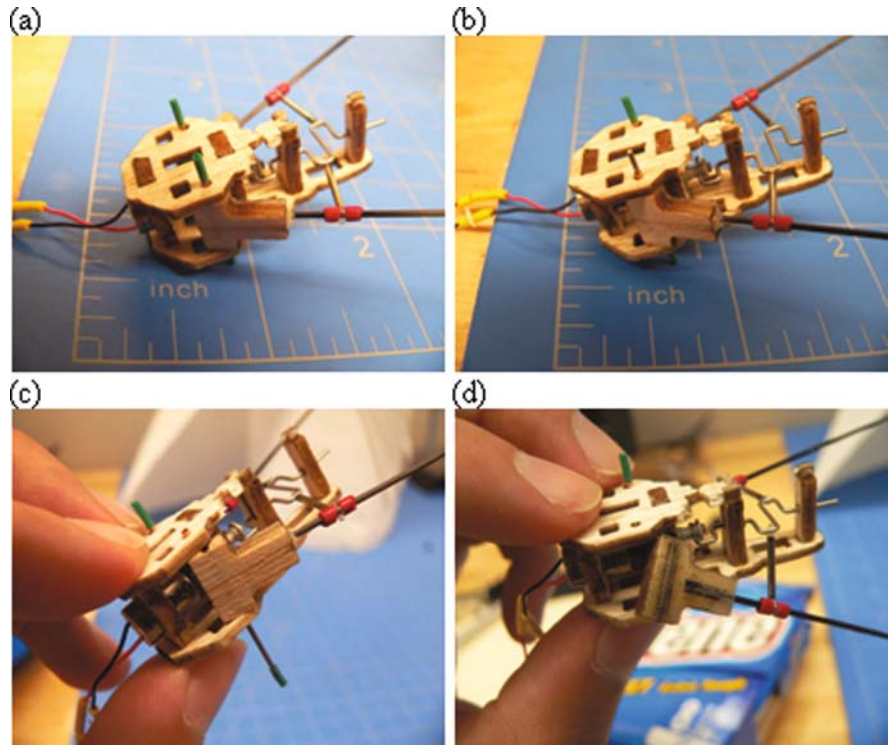

Fig. 13.10 New design of the wing hinge. (**a**–**d**) The sequence in which a wing can be easily removed for repair or modifications

maneuverability is a high priority. However, for applications where stationary hovering and slow maneuvering flight are desired, such an approach may be of interest. The sails also increase the machines' susceptibility to gusts of wind. While in the real world this approach is not likely ideal, in the emerging field of untethered hovering flapping micro-air vehicles, where weight is of utmost concern, passive stability provides a simple and lightweight solution for tuning and testing the thrust portion of the design, which is the crux of the field at this point.

The stabilization dynamics are governed by two sails, which cause it to act like a damped pendulum. In order to intuitively understand the dynamics, think of the machine as a mass on a rod. If we were to place a pivot point below the mass, it would act as an inverted pendulum and thus be unstable. Placing the pivot point above the mass, however, causes it to act as a pendulum, which in the presence of damping will be stable. The pivot point is determined by the center of the drag forces caused by the sails. If this pivot point is above the center of mass, the system will be stable. In order to verify the stability of the model we used a first-order approximation of the free body diagram in Fig. 13.11. The stability of the device has been verified by its ability to recover from arbitrary launch orientations, including upside-down zero-velocity initial conditions that are typically very difficult for most aircraft's to recover from (including helicopters).

Using a first-order approximation of the system dynamics we can show its stability mathematically. The free body diagram in Fig. 13.11 yields the following equations:

$$\sum Forces = F_t\mathbf{j}' - F_{DW}\mathbf{j}' - Mg\mathbf{j} - F_{D1}\mathbf{i}' - F_{D2}\mathbf{i}' = M\mathbf{a}$$

$$\sum Moments = -cM\sin\theta + aF_{D1} - bF_{D2} = I\ddot{\theta}$$

For the simplified system, $I = Mc^2$. The key to understanding how the stability works lies in the center of rotation, which is the point where the drag induced from the two sails during rotation is balanced, which imposes the constraint, $aF_{D1} = bF_{D2}$ (note a+b=length of the machine, providing two equations to solve for a and b). In order to analytically examine the system we approximated the drag

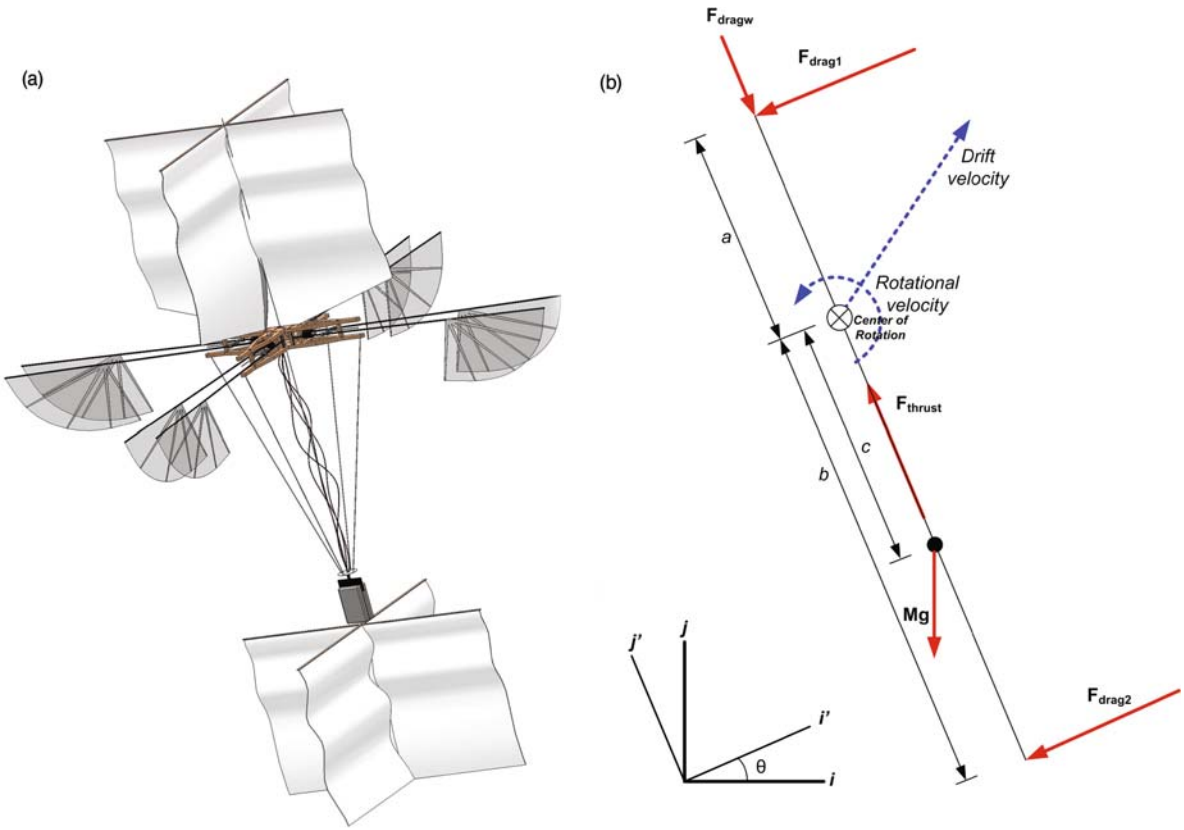

Fig. 13.11 Passive stabilization mechanism. (**a**) CAD diagram and (**b**) free body diagram of perturbed system. The hovering machine has thrust exactly equal to its weight. Small perturbations will cause an imbalance in forces and the machine may begin to rotate and drift. The *top* and *bottom* sails act as dampers, producing a restoring force in the presence of a drift or rotational velocity. These two dampers determine a rotation point for the machine. If the rotation point is above the center of mass, the machine will be stable, similar to a damped pendulum. A damping along the axis is due to a damping factor from the flapping wings

force as being linearly proportional to the velocity. This approximation is reasonable for low translational velocities, which is true in the hovering case that we are interested in. Next we used a small angle approximation to simplify the analysis.

The drag forces can be written as follows:

Drag on the flapping wings: $F_{DW} = d_w \dot{y}'$
Drag on the top sail: $F_{D1} = d_1(\dot{x}' - a\dot{\theta})$
Drag on the bottom sail: $F_{D2} = d_2(\dot{x}' + b\dot{\theta})$,

where $d_{1,2,w}$ are of the form $\frac{1}{2}\rho C_d A$, ρ is the fluid density, C_d is the drag coefficient, and A is the cross-sectional area.

In order to determine the stability of the system we can put it into state space, and examine the eigenvalues, in addition to some test case scenarios. The response was examined for an initial 10° offset of the tilt angle (Fig. 13.12). It can be concluded that for stability the center of rotation defined by the two sails as above needs to be above the center of mass. Using the following values we simulated the system in Matlab:

$d_1 = 0.03142$ kg/s (based on $0.5 * rho * C_d * A$)
$d_2 = 0.02244$ kg/s (based on $0.5 * rho * C_d * A$)
$d_w = 0.01$ kg/s (arbitrary, but has no effect on stability provided it is > 0)
$a = 0.191$ m (distance from d_1 to the center of rotation, defined by $aF_{D1} = bF_{D2}$)
$b = 0.268$ m (distance from d_2 to the center of rotation, defined by $aF_{D1} = bF_{D2}$)
$M = 0.025$ kg (machine mass)
$g = 9.8$ m^2/s (acceleration due to gravity)

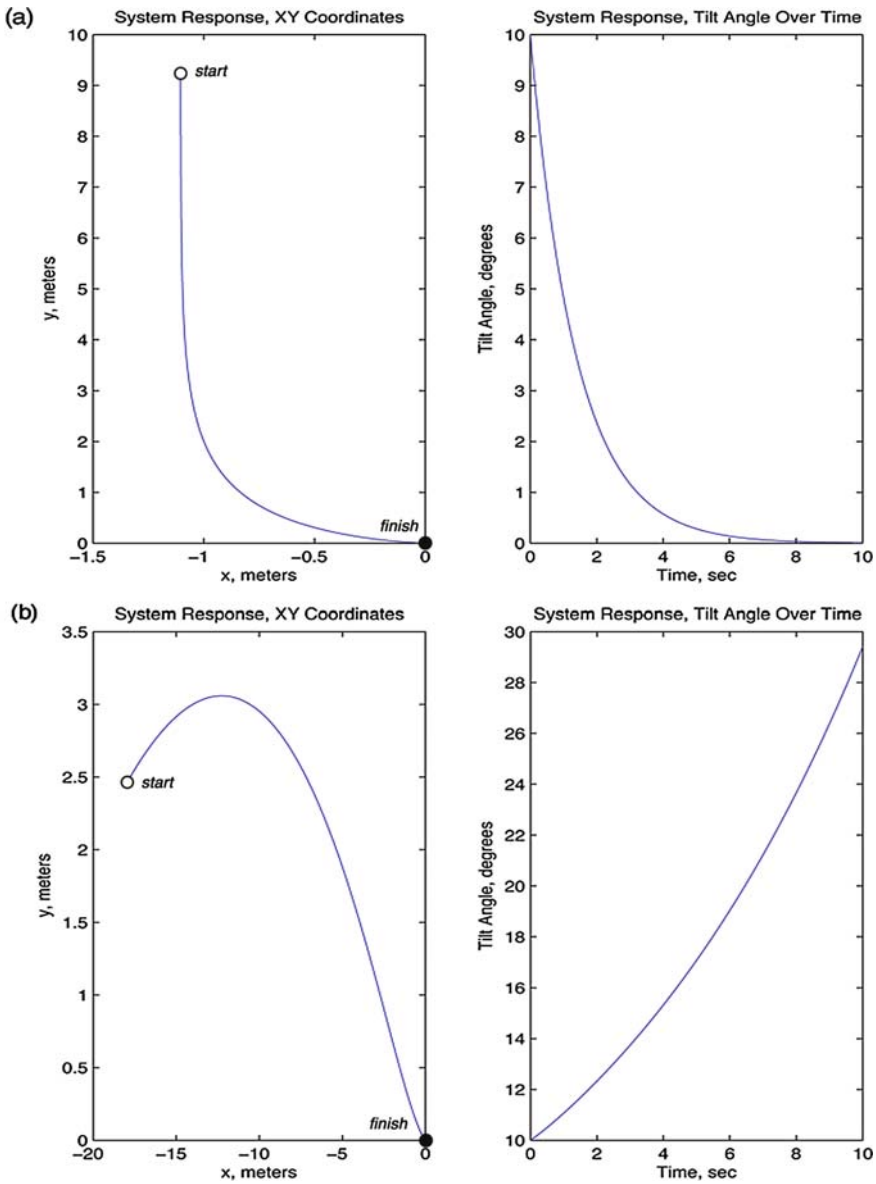

Fig. 13.12 System response for (a) a stable system, with the center of mass located below the pivot point. The system started at (0,0) with a tilt angle of 10° at time=0 (open circle) and proceed to stabilize, ending at the *black circle*. (b) unstable system response with the center of mass located above the pivot point. The system started at (0,0) with a tilt angle of 10° at time=0 (*open circle*) and did not stabilize, ending at the *black circle*

$F_t = 1.05 * \mathrm{M} * \mathrm{g}$ (thrust slightly higher than the hovering condition)

$c = 0.00833$ m (distance from center of rotation to center of mass)

Analyzing this system yields the eigenvalues: {0, −1589.1, −2.2, −0.7, 0, −0.4}. The two zero-value eigenvalues are due to the rigid body modes. This can be verified by adding a spring in the x and y dimensions, causing all the eigenvalues to be negative.

13.5 Performance Results

The design can be operated under a variety of configurations, depending on the need for longer flight times or increased payload capacity for tools such as sensors and cameras. Power, lift, and flapping frequency were measured using a digital multimeter, a scale, and strobe light (Fig. 13.2). Under maximum lift conditions the craft operates at a Reynolds Number of roughly 8,000.

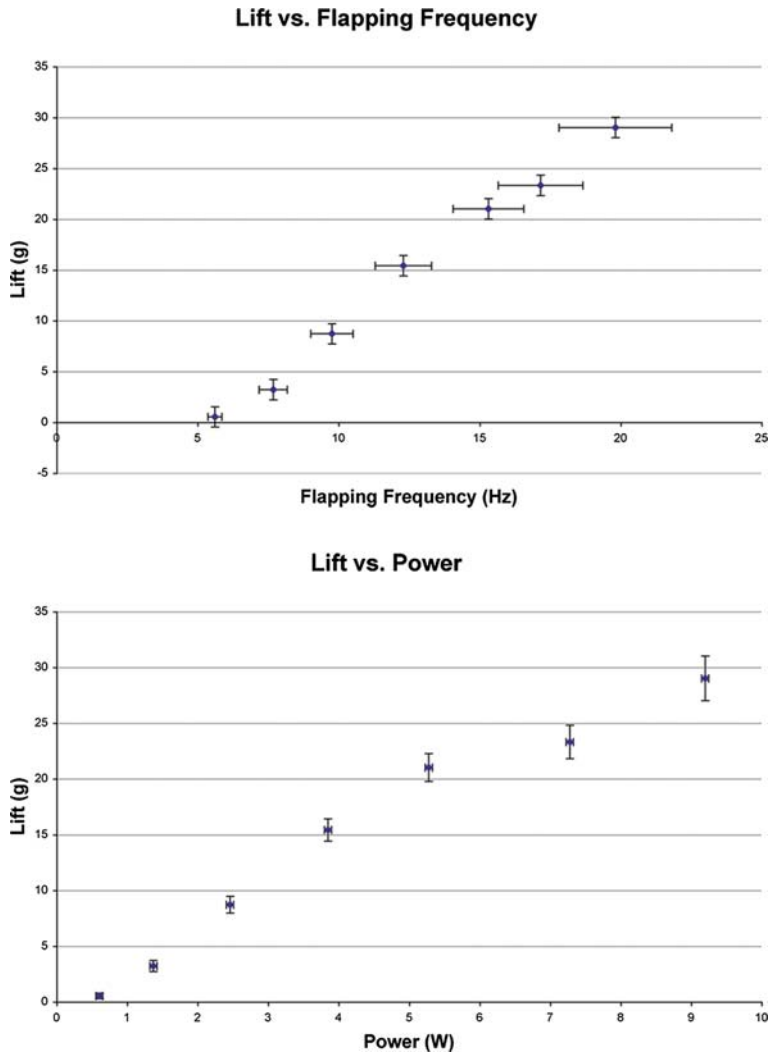

Fig. 13.13 Operating characteristics. Lift and frequency for various power arrangements. The nonlinearity at 7.5 W is likely due to a second oscillatory mode resembling a standing wave that appeared at this power. Furthermore the motor efficiency becomes nonlinear as the power increases. We operated the machine just below this point, at 6.9 W

Our current mode of operation uses two 3.7 V, 90 mA h Li-Poly batteries in series to provide a nominal output voltage of 7.4 V. At these voltages the flapping transitions into a second oscillatory mode: a standing wave with nearly zero lift production. In order to minimize this effect we implemented a 0.8½ resistance to reduce the voltage. This also reduced the stress on the motors and lowered the maximum height achieved. Operating conditions were measured to 6.5 V at 1.07 A for a total lift of 25 g capable of 33 s flight. The poor performance is likely due to the motors being driven far beyond their recommended operating characteristics, lack of a voltage regulator, and unoptimized wing structure (see Sect. 13.5.1) (Fig. 13.13).

13.5.1 Future Design Changes

In order to improve the machines performance there are a number of issues that need to be addressed. First, several of the components (motors, batteries, and wires) are being operated at a much higher power than is recommended. With the addition of an efficient voltage regulator and by minimizing the length and amount of wiring we can further reduce wasted power. Beyond component optimization the wing shape and materials need to be examined more carefully. During our design process we systematically tried various wing shapes, sizes, and material properties, yet were unable to find a simple method to help us optimize the wing

shape. Once we found the presented design to work we moved on to other areas of the machine. The first step is to design reliable experiments for measuring lift with systematic changes to the wings. This is made difficult due to the fact that the machines' flapping characters change when it is tethered to a stiff stand. We will need to investigate a number of attributes including size, geometry, aspect ratio, mass distribution, flexibility, and flexibility distribution. Having a more flexible trailing than leading edge may help increase lift by reducing the formation of trailing edge vortices which destroy the lift enhancing leading edge vortices [14]. Different mechanisms of flapping can also be explored. Currently, the motor is attached directly to the wings simulating a direct method of flapping. Perhaps indirect mechanisms of flapping as observed in the *Drosophila* could be used. *Drosophila* expands and contracts its thorax to produce its flapping motion, using elastic energy storage for increased efficiency. Perhaps the use of a more biomimetic actuator would further improve our efficiency.

We also began to explore altitude control as a first step into implementing active control of the flapper by controlling each motor individually. We used a four-channel receiver from Plantraco (Micro9-S-4CH 1.1 g Servo Rx w/ESC) and a Plantraco transmitter (HFX900 M2). We converted Blue Arrow 2.5 g servos from positional control to speed control to make use of the four-channel receiver. The difficult design constraint here was that we needed four-channels of control, while most lightweight electronics are made for two–three control outputs. On testing, we found that the performance of the modified servos was unstable. There was also an appreciable drop in voltage from the batteries to the motors. This resulted in poor lift generation. Our next approach was to connect the four motors in parallel and wire them to the throttle output which had a 2 A output. (At this point we could have changed the design to use a different receiver and transmitter with just a single channel.) With an external power source of 7 V at maximum throttle, the receiver would consistently let out a sharp beep and the motors would start to reduce their flapping frequency as opposed to maintaining a frequency suitable for substantial lift generation. This could be due to the overloading of the throttle which was designed for only one motor. Here we are loading it with four motors. Control could also be achieved by altering the stroke plane as opposed to altering the power of the motors. Potentially, the four connections of the module connector to an individual module could be replaced with material that mimics muscle. Looking at Fig. 13.8a, if the connector arms are replaced with an actuator that contracts like a muscle, the stroke plane can be tilted when the "artificial muscle" contracts. Shape memory alloys (SMAs) and piezo actuators come to mind. However, SMAs generate substantial amounts of heat and piezo actuators require a high voltage to achieve appreciable strain. Therefore, issues of weight and input power need to be addressed before such an artificial muscle can be used in the flapper.

13.6 Conclusion

While the performance of the machine presented here needs to be improved, it demonstrates several design considerations relevant to others interested in stable and controllable hovering flapping MAVs. The quad-flapper design allows for active control using the thrust from the wings, rather than additional rudders and actuators. Since our machine operates within the same aerodynamic flow regime of insects, these design principles should scale favorably to insect-sized machines. While for real-world applications active control is critical, in designing and optimizing the thrust portions of small-scale flapping MAVs the use of sails for passive stability may prove to be much simpler than trying to build an active controller small enough that it can be carried on board. Ultimately we hope hovering flapping flight will open the door to new applications and provide further insight into the mechanisms underlying insect and hummingbirds remarkable flying abilities.

Acknowledgments We would like to thank our funding sources for supporting this project, including Cornell Presidential Research Scholars, the NASA Space Consortium, and the NASA Institute for Advanced Concepts.

References

1. Arrow, B.: Wing bird rc flying bird (2005). http://flyabird.com/wingbird.info.html
2. Berman, G., Wang, J.: Energy-minimizing kinematics in hovering insect flight. Journal of Fluid Mechanics **582**, 153–168 (2007)

3. Chronister, N.: The ornithopter zone – fly like a bird – flapping wing flight. http://www.ornithopter.org/
4. Combes, S.A., Daniel, T.L.: Into thin air: contributions of aerodynamic and inertial-elastic forces to wing bending in the hawkmoth manduca sexta. The Journal of Experimental Biology **206**, 2999–3006 (2003). 10.1242/jeb.00502. http://jeb.biologists.org/cgi/content/abstract/206/17/2999
5. Dalton, S.: Borne on the Wind. Reader's Digest Press, New York (1975)
6. DeLaurier, J., SRI/UTIAS: Mentor project (2005). http://www.livescience.com/technology/041210_project_ornith%opter.html
7. Dickinson, M.H., Lehmann, F.O., Sane, S.P.: Wing rotation and the aerodynamic basis of insect flight. Science **284**, 1954–1960 (1999). 10.1126/science.284.5422.1954. http://www.sciencemag.org/cgi/content/abstract/284/5422/1954
8. Dickson, W., Dickinson, M.H.: Inertial and aerodynamic mechanisms for passive wing rotation. Flying Insects and Robotics Symposium, p. 26 (2007)
9. Ellington, C.: The novel aerodynamics of insect flight: applications to micro-air vehicles. The Journal of Experimental Biology **202**, 3439–3448 (1999). http://jeb.biologists.org/cgi/content/abstract/202/23/3439
10. Ellington, C.P., van den Berg, C., Willmott, A.P., Thomas, A.L.R.: Leading-edge vortices in insect flight. Nature **384**, 626–630 (1996). 10.1038/384626a0. http://dx.doi.org/10.1038/384626a0
11. Fearing, R., Wood, R.: Mfi project (2007). http://robotics.eecs.berkeley.edu/ronf/MFI/index.html
12. Jones, K., Bradshaw, C., Papadopoulos, J., Platzer, M.: Bio-inspired design of flapping-wing micro air vehicles. Aeronautical Journal **109**, 385–393 (2005)
13. Keennon, M., Grasmeyer, J.: Development of two mavs and vision of the future of mav design. 2003 AIAA/ICAS International Air and Space Symposium and Exposition: The Next 100 Years (2003)
14. Lehmann, F.O.: When wings touch wakes: understanding locomotor force control by wake wing interference in insect wings. The Journal of Experimental Biology **211**, 224–233 (2008). 10.1242/jeb.007575. http://jeb.biologists.org/cgi/content/abstract/211/2/224
15. Lehmann, F.O., Sane, S.P., Dickinson, M.: The aerodynamic effects of wing-wing interaction in flapping insect wings. The Journal of Experimental Biology **208**, 3075–3092 (2005). 10.1242/jeb.01744. http://jeb.biologists.org/cgi/content/abstract/208/16/3075
16. Lentink, D., Team, D.: Delfly (2007). http://www.delfly.nl/
17. Michelson, R.: Entomopter project (2003). http://avdil.gtri.gatech.edu/RCM/RCM/Entomopter/EntomopterPro%ject.html
18. Michelson, R., Naqvi, M.: Extraterrestrial flight. Proceedings of von Karman Institute for Fluid Dynamics RTO/AVT Lecture Series on low Reynolds Number Aerodynamics. Brussels, Belgium (2003)
19. Wang, J.: Dissecting insect flight. Annual Review of Fluid Mechanics **37**, 183–210 (2005). http://arjournals.annualreviews.org/doi/abs/10.1146/annurev.f%luid.36.050802.121940?cookieSet=1&journalCode=fluid
20. Woods, M.I., Henderson, J.F., Lock, G.D.: Energy requirements for the flight of micro air vehicles. Aeronautical Journal **105**, 135–149 (2001)
21. Wowwee: Wowwee flytech dragonfly toy 2007). http://www.radioshack.com/product/index.jsp?productId=2585632%&cp&cid=